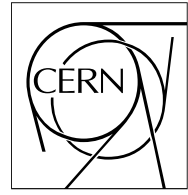


The Compact Muon Solenoid Experiment

CMS Note

Mailing address: CMS CERN, CH-1211 GENEVA 23, Switzerland



Sep 27, 2005

Changes in light yield from the CMS ECAL during LHC operation

D.J.A. Cockerill

Rutherford Appleton Laboratory, UK

Abstract

The changes in light yield from the lead tungstate crystals in the CMS ECAL during LHC operation have been estimated for the barrel and endcap regions of the detector. The formation of colour centres and the change in light yield have been simulated at hourly intervals for one year of LHC operation, for startup, low, high and SLHC luminosities (10^{33} , $2 \cdot 10^{33}$, 10^{34} and $10^{35} \text{ cm}^{-2} \text{ sec}^{-1}$ respectively). The consequent demands on the ECAL monitoring system, the effect on the noise and performance, and the consequences for the ECAL trigger are discussed.

1: Introduction

The CMS Electromagnetic calorimeter (ECAL) at the LHC comprises a Barrel (EB) and two Endcap (EE) detectors containing 61200 and 14648 lead tungstate crystals, respectively. The EB subtends a pseudorapidity range from $|\eta| = 0$ to 1.48. The EE subtends a pseudorapidity range from $|\eta| = 1.48 - 3.0$ [1].

The calorimeter is designed to have excellent performance with high precision energy resolution resulting in excellent mass resolution for the detection of new particles such as Higgs bosons. Energy resolutions of 0.55% has been achieved at a test beam for electrons at an energy of 100 GeV [2]. At high energies the calorimeter resolution is expected to be limited by the calorimeter constant term and intercalibration errors, at a combined level of $\sim 0.4 - 0.5\%$.

In order to maintain the performance of the detector it is important to minimise any effects that might degrade the energy resolution, and to keep the impact of such effects on the energy resolution to 0.3% or less. One such effect is the formation of colour centres in the crystals caused by ionising radiation. The colour centres change the transparency of the crystals, particularly near the lead tungstate emission peak at 420nm [3]. This leads to a change in light yield which must be corrected for.

The level of colour centre creation is dependant on the the number of potential colour centre sites within the crystals. The sites are activated by the ionising particles generated by the LHC. The number of created sites is dependant on the local dose rates within the crystals. The behaviour of the colour centres with time are governed by intrinsic time constants for their creation and annihilation.

The transparency of the lead tungstate crystals will be monitored with a laser system. Laser light at 440nm will be injected into the front of EB crystals, and into the back of EE crystals, via quartz fibres. The laser signals are monitored with PN diodes. The normalised laser data, using the PN diode signals, will be used to track crystal transparency with time. The transparency data will be used to provide corrections to the measured energies in the detector [4].

The crystals for the ECAL are produced at two sites, Bogoroditsk (BTCP), Russia and the Shanghai Institute of Ceramics (SIC), China. BTCP is expected to provide $\sim 95\%$ of the crystals in the EB and $\sim 80\%$ of the crystals in the EE.

This note quantifies the level of colour centre formation and the consequent level of light yield loss that may be expected from lead tungstate crystals at the LHC. The note outlines the constraints on the ECAL monitoring system if it is to adequately follow the detector in real time at the LHC, and the energy equivalent noise targets that are required in the detector before LHC operation commences.

Light yield losses which may occur due to heavily ionising hadronic interactions are not considered in this paper [5].

2: The simulation

The various processes which contribute to colour centre formation in a crystal are discussed separately. These factors are then folded together to replicate the environment at the LHC. Amongst these factors are:

- the dynamics of crystal colour centre creation
- the total number of potential colour centre sites available within a crystal
- the induced absorption and light yield loss as a function of dose rate
- the profile of the dose and the dose rate as a function of depth in a crystal
- the LHC luminosity profile with time
- the dose rates in a crystal as a function of time
- the net crystal light yield as a function of time.

3: Crystal dynamics

Colour centres are created in PbWO_4 under the influence of ionising radiation. The density of colour centres at any time is dependant on the rate of creation of the centres and the rate of their subsequent annihilation.

The rate of formation of a colour centre i is usually given by $b_i R$ (h^{-1}), where b_i is a constant in Gy^{-1} and R is the local dose rate in Gy/h . The annihilation rate is given by a constant a_i (h^{-1}). The differential change of colour centre density when both processes coexist can be written as

$$dD = \sum_{i=1}^n \left\{ -a_i D_i + (D_i^{all} - D_i b_i) R \right\} dt \quad (1)$$

where D_i is the density of colour centre i in the crystal and the summation goes over all types of centre [6]. The solution to this equation is

$$D = \sum_{i=1}^n \left\{ \frac{b_i R D_i^{all}}{a_i + b_i R} [1 - e^{-(a_i + b_i R)t}] + D_i^0 e^{-(a_i + b_i R)t} \right\} \quad (2)$$

where D is the number of activated colour centres present in the crystal at time t , D_i^{all} is the total density of the potential traps related to colour centre type i and D_i^0 is their initial density at $t = 0$. The colour density in equilibrium (D_{eq}) thus depends on the dose rate (R).

$$D_{eq} = \sum_{i=1}^n \frac{b_i R D_i^{all}}{a_i + b_i R} \quad (3)$$

This dependence on dose rate has been observed in many PbWO_4 samples [7].

4: Crystal dynamics used for the simulation

Equations (1) - (3) are multi-parameter and it is difficult, if not impossible, to extract all of the terms for each type of colour centre from the data taken from existing test bench setups for the appraisal of PbWO_4 during and after irradiation. However, many PbWO_4 crystals appear to be adequately described by a single colour centre type over short time periods of $\sim 24\text{h}$ together with a second colour centre which anneals with a much longer time constant. Such a crystal is CMS mass production crystal 4005 from BTCP.

Crystal 4005 was irradiated at the GIF irradiation facility at CERN [8]. The crystal was irradiated laterally, with a uniform dose delivered along its length. Its behaviour under irradiation is shown in Fig. 1. The longitudinal transmission through the crystal was measured with a blue

LED before, during and after irradiation at 0.15 Gy/h . During irradiation the decrease of the LED signal can be described by a single exponential with a time constant of 3.96h at 0.15 Gy/h. After irradiation the increase in the LED signal, due to crystal annealing, can be partly described by a single exponential with a time constant of 18.55h [9].

The annealing does not bring the crystal back to the initial level of LED signal. There is a residual loss of 1% (30% of the total light yield loss) which appears to have a much longer time constant for annealing. This is relatively common in irradiation data from lead tungstate crystals. For this simulation only the 18.55h annealing time is used and the crystal is allowed recover completely. The consequences of the long annealing time constants are discussed separately in section 11.

Fig. 2 shows the annealing times for a set of 9 BTCP crystals following irradiation at 350Gy/h for a total of 400Gy [10]. The crystals have annealing times from 20 to 35h. Crystal 4005 is indicated on the plot and is similar to the crystals with annealing times of ~20h.

By contrast, crystals from SIC have a flat distribution of annealing times which vary from ~20h to 200h [10]. For comparison with the other BTCP crystals and with the SIC crystals with long time constants, simulations have also been carried out with annealing times of 30, 40 and 100h, but with the colour centre creation coefficient, b , obtained from crystal 4005.

Assuming that the different colour centre dynamics can be approximated by an average behaviour, b , for the rate of creation, and an average behaviour, a , for the rate of annihilation then equation (2) simplifies to

$$D = \frac{bRD^{all}}{a + bR} [1 - e^{-(a + bR)t}] + D^0 e^{-(a + bR)t}, \quad (4)$$

where D^{all} is the total number of potential colour centres available within the crystal, R is the dose rate in Gy/h and D^0 is the number of pre-existing colour centre sites.

Table 1 shows the values for a and b obtained from the fits to the data for crystal 4005, where $(a+bR)^{-1} = 3.96$ h.

Table 1: Colour centre dynamics for crystal 4005

	Dose Rate (Gy/h)	Time constant (h)	Coefficient
Colour centre creation	0.15	3.96	$b = 1.32 \text{ Gy}^{-1}$
Colour centre annealing	-	18.55	$a = 0.054 \text{ h}^{-1}$

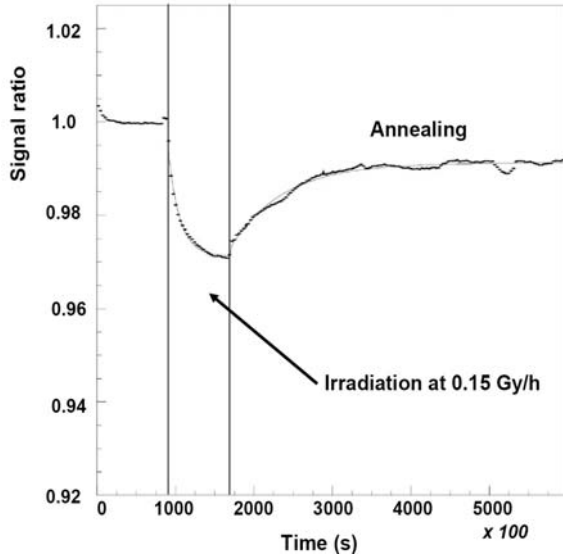


Figure 1.

The LED signal measured for PbWO_4 crystal # 4005 before, during and after irradiation at 0.15Gy/h.

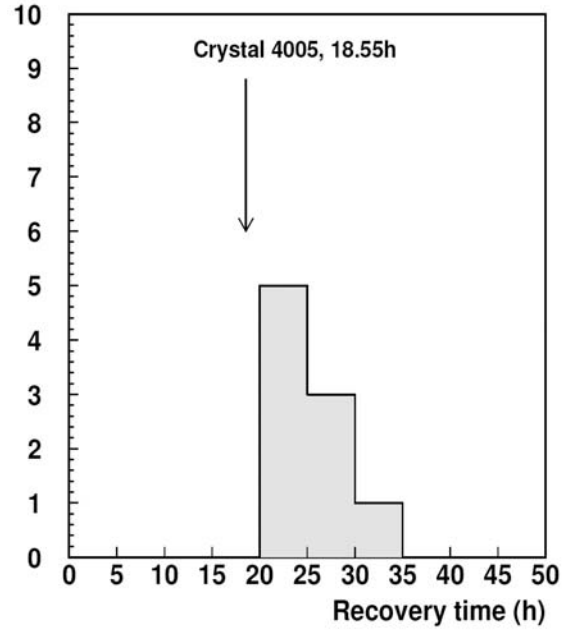


Figure 2.

The distribution of light yield recovery times for 9 BTCP crystals measured after irradiation at 350Gy/h for 1.1h. The recovery time for crystal #4005 is indicated by the arrow.

The evolution of equation (4) depends upon the total number of potential colour centre sites available within a crystal, D^{all} . This information is obtained from the irradiation of crystals at high dose rates and is discussed in the next section.

The characteristic times for colour centre creation, using the data from crystal 4005, are shown in Fig. 3 as a function of η , for the dose rate at dose maximum, for startup, low, high and SLHC (Super LHC) luminosity running.

In the Barrel ($|\eta| < 1.48$) the time constants for colour centre creation range from 10 to 2 hours for nominal startup, low and high luminosities. In the Endcap the colour centre creation times decrease approximately linearly with eta and are less than 30 minutes for the nominal low and startup luminosities and only 4 minutes at high luminosity, at $|\eta| = 2.9$. At the SLHC the colour centre creation times decrease from 25 minutes at $|\eta| = 0$ to only 20 seconds at $|\eta| = 2.9$.

5: Total number of potential colour centre sites, D^{all}

The total number of potential colour centre sites, D^{all} , can be found by uniformly laterally irradiating crystals at very high dose rates [12]. Typically these rates are ~ 240 Gy/h and are applied for ~ 2 h to ensure that the crystals have come to equilibrium. In comparison, the highest dose rate in the CMS electromagnetic calorimeter at high luminosity ($10^{34} \text{ cm}^{-2} \text{ s}^{-1}$) is 15 Gy/h at the dose maximum at $\eta = 3$.

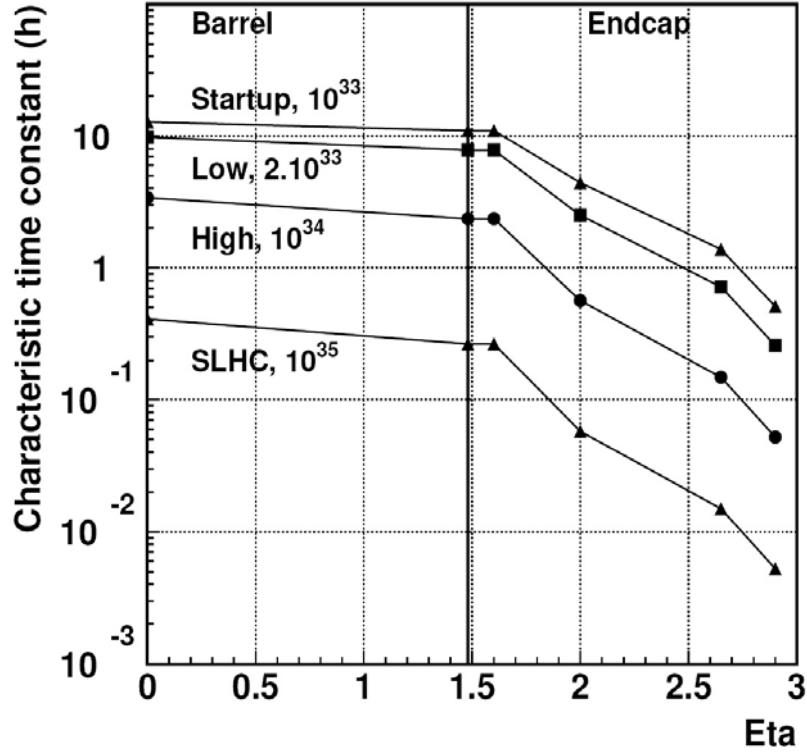


Figure 3.

Characteristic colour centre creation times as a function of η , for the dose rate at dose maximum, for startup, low and high luminosity running.

D^{all} can be measured as the longitudinally induced absorption of light at 420nm, the $PbWO_4$ emission peak, following irradiation. These measurements can be performed quickly and accurately with a spectrophotometer by shining light down the length of the crystal. Most of the crystals measured for CMS are characterised in this way. The induced absorption, α (m^{-1}), is found from $I = I_0 \exp(-x\alpha)$, where I is the measured light intensity following irradiation, I_0 the light intensity before irradiation and x the length of the crystal exposed to the beam of light.

D^{all} can also be quantified in terms of the light yield loss following irradiation. These values are required for the simulation in order to evaluate the effects on detector performance. However the measurements of light yield loss, involving a Co^{60} setup, are time consuming and relatively few crystals have been measured in this way.

A set of 23 EE crystals produced at BTCP were measured for both induced absorption and light yield loss [13]. The data are shown in Fig. 4. These data have been used to convert the extensive induced absorption data, obtained from many crystals, to equivalent light yield loss. A fit was made to the data assuming that the light yield loss can be expressed as

$$LY \text{ loss (\%)} = 100(1 - \exp(-xa)) \quad (5)$$

where the light yield is related to the initial light yield by $LY = LY_0 \exp(-xa)$, x is an effective path length and a is the measured induced absorption. A value for x of 53.6 cm was found from the fit.

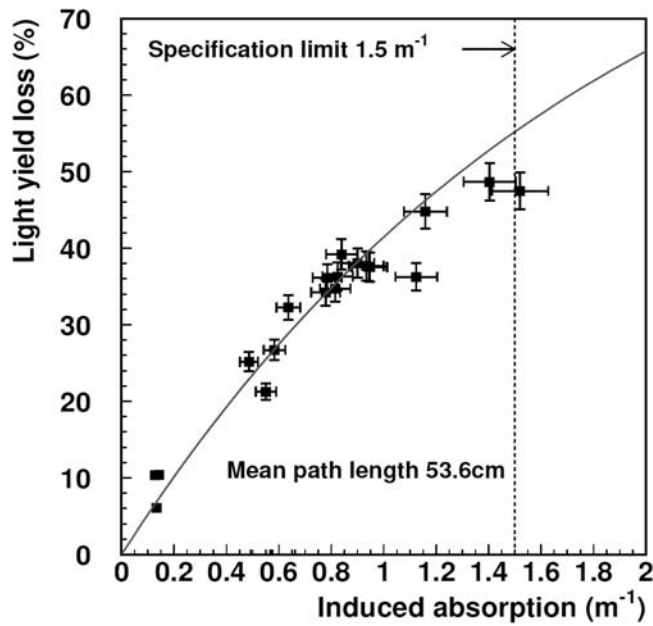


Figure 4.

The correlation between induced absorption and light yield loss for 23 EE crystals from BTCP. The fit to the data gives an effective path length of 53.6 cm. At 1.5 m^{-1} the light yield loss is 50%.

The induced absorption data for 677 crystals, after lateral irradiation at 240Gy/h for 2h, are shown in Fig. 5 [11]. The distribution has a mean value of 0.73 m^{-1} and has a cut-off at 1.5 m^{-1} , the technical specification limit for the acceptance of crystals in CMS.

Using equation (5), the induced absorptions measured in Fig. 5 can be converted to equivalent light yield losses. The resultant distribution is shown in Fig. 6. The mean value for D^{all} , expressed as a light yield loss, is 31.6%. This is the mean value to be expected in crystals at very high dose rate under uniform lateral irradiation. The rms for the distribution is 11%. The data indicate that crystals are likely to suffer light yield losses of between 20% and 40% at very high dose rate, with a few crystals suffering light yield losses of up to 55%.

The relationship between induced absorption and light yield loss is different for SIC crystals. An effective path length of $x = 35.3\text{cm}$ was found for 30 SIC crystals, using equation (5) in comparison to the 53.6cm found for BTCP crystals. The SIC crystals had a 42% light yield loss for an induced absorption of 1.5m^{-1} , in comparison to a 55% light yield loss for the BTCP crystals.

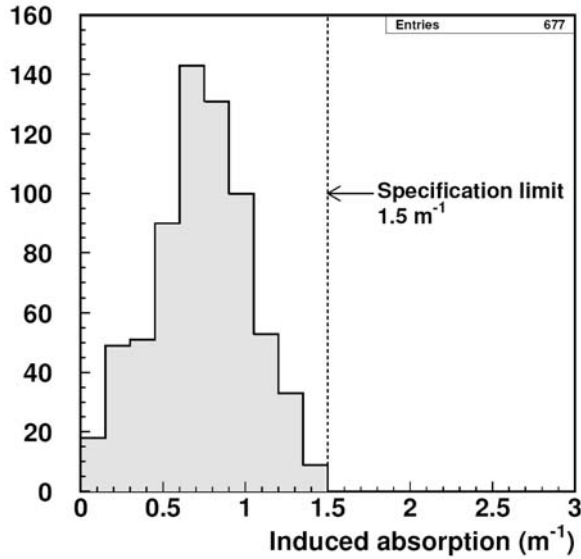


Figure 5.

The induced absorption measured at 420nm for 677 barrel crystals following an exposure of 240 Gy/h for 2h. The mean value is 0.73 m^{-1} with an rms of 0.3 m^{-1} .

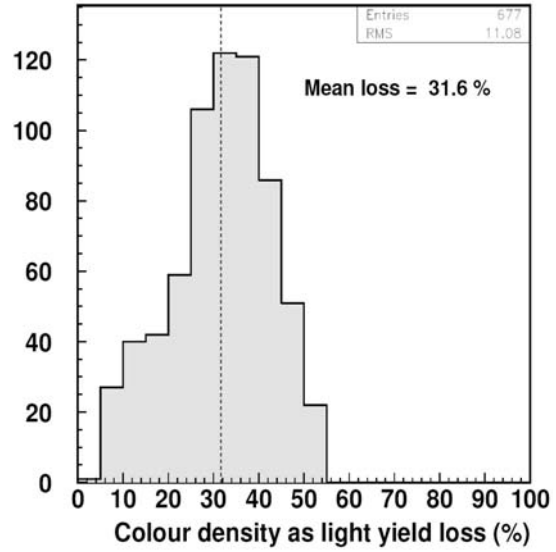


Figure 6.

The distribution of D^{all} expressed as the percentage light yield loss, for 677 barrel crystals calculated from the induced absorption data shown in Fig. 5.

6: Uniform irradiation and the dose profile at LHC

The studies of induced absorption and light yield loss in section 5 were undertaken by performing uniform lateral irradiations of the crystals [12]. At LHC the dose rates are not uniform along the lengths of the crystals. An average light yield loss must be calculated from the losses arising from each section along a crystal.

Detailed measurements of light yield loss as a function of position along a crystal have been carried out using a Co^{60} source and an HPMT (Hybrid Photomultiplier tube) [14]. The data are shown in Fig. 7 following five hours of uniform lateral irradiations of a crystal at 0.15, 0.45, 0.5 and 15Gy/h, with one day between each irradiation. The Co^{60} measurements were carried out in steps of 1cm along the crystal.

The measured light yields are flat along the crystals, for each dose rate, to a level of 0.7% r.m.s., apart from the data following the 0.45Gy/h irradiation which were flat to 1.3% r.m.s.. There is a consistent small rise in light yield of ~1% near the photo-detector end.

The data for uniform lateral irradiation show that the collection of scintillation light is uniform from all points along the crystal. The absorption losses in each section contribute equally to the overall light yield loss. This is true up to the 21% light yield losses measured at 15 Gy/h.

For the case of non-uniform irradiation at the LHC the overall light yield loss is calculated from the mean of the colour centre densities created in each section along the crystal.

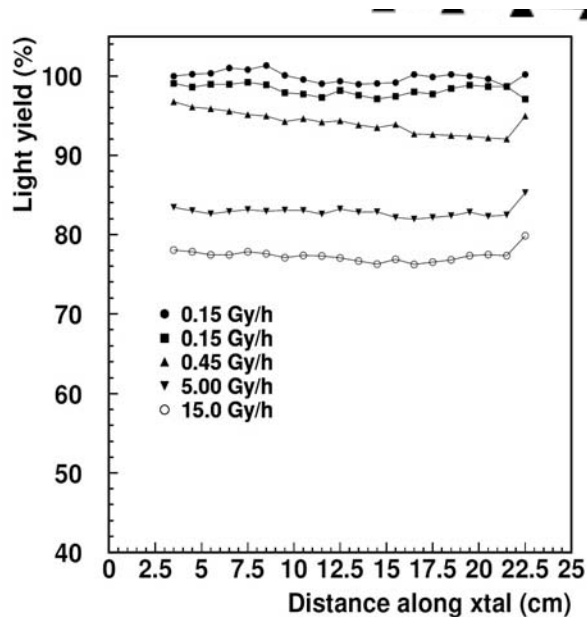


Figure 7.

The light yields measured along an Endcap crystal using an HPMT photodetector following uniform lateral irradiations for 5h at 0.15, 0.45, 5 and 15 Gy/h. The HPMT was mounted at the rear of the crystal at 22cm.

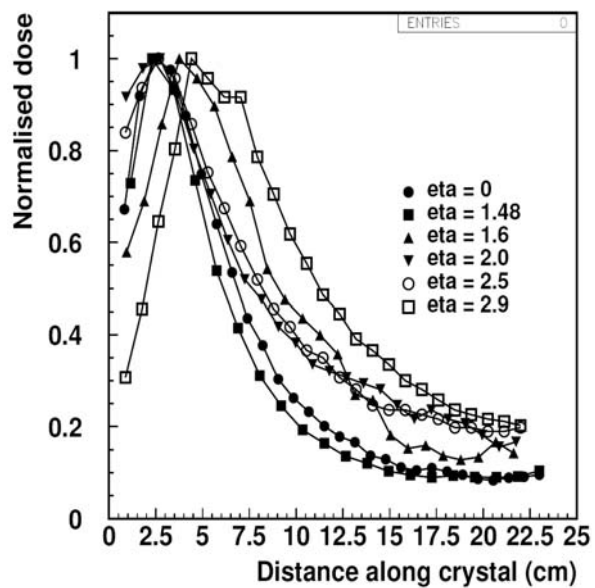


Figure 8.

The dose profiles in crystals, normalised to the dose maximum, for the barrel at $\eta = 0$ and 1.48 and for the endcaps at $\eta = 1.6, 2.0, 2.5$ and 2.9.

The profile of the dose delivered along the length of the crystals in the CMS electromagnetic calorimeter is required in order to calculate dose rates at each point along the crystals during LHC operation. The dose profiles at six values of eta from $\eta = 0.0$ to $\eta = 2.9$ are shown in Fig. 8 normalised to the maximum delivered dose. The data are taken from the ECAL TDR, Figs. A4 and A5, which show the integrated doses delivered after 10 years of LHC operation ($5 \cdot 10^5 \text{ pb}^{-1}$) [1]. The profiles extend to 23cm for barrel crystals and to 22cm for endcap crystals.

The delivered dose is less than 40% of the maximum delivered dose for depths in the crystals beyond 10-12 cm. At the back of the crystals the dose is only 10-20% of the maximum delivered dose.

7: LHC Luminosity

The instantaneous LHC luminosity governs the dose rate delivered to crystals in the CMS ECAL. The LHC luminosity decreases from the initial luminosity at the start of fill due to

beam-gas scattering, machine losses and beam-beam losses from p-p interactions [15]. The variation of luminosity with time can be expressed as:

$$L(t) = L_0 \left(\frac{N(t)}{N_0} \right)^2$$

$$\text{where } N(t) = \frac{N_0 e^{-t/t_g}}{1 + \frac{t_g}{t_{bb}} (1 - e^{-t/t_g})}$$

For the nominal LHC design parameters and two experiments, $t_g = 43\text{h}$ and $t_{bb} = 40\text{h}$. The machine filling is expected to take 10h and running to take place for 14h for each fill, giving one fill cycle per day [16]. The resultant luminosity curve as a function of time is shown in Fig. 9. The luminosity drops essentially exponentially with a lifetime of 11.5h to ~30% of its initial value by the end of the fill.

In addition to the variation of luminosity during a fill there are also variations from fill to fill. Fill to fill variations are expected to be between 100% and 30% of the target luminosity. Fig. 10 shows the initial fill values randomly generated for one LHC year corresponding to 3 periods each with 60 fills with a maximum luminosity of $10^{34} \text{ cm}^{-2} \text{ s}^{-1}$. Each period is separated by 10 days.

8: Crystal light yield in real time at the LHC

Since the luminosity, and therefore the dose rate, are not constant at the LHC, equation (4) must be modified to incorporate the time dependance of the dose rate. In the simulation the LHC luminosity is approximated by a set of constant luminosity steps, each of one hour duration, as shown in Fig. 9.

The dose rate at the dose maximum in the crystals, at a luminosity of $10^{34} \text{ cm}^{-2} \text{ s}^{-1}$, is shown in Fig. 11 as a function of η . The fit to the data is from $\eta = 1.6$ to $\eta = 2.9$. In the EB the rate rises slowly from 0.18 Gy/h at $\eta = 0$ to 0.29 Gy/h at $\eta = 1.48$. In the EE the rate increases exponentially and is nearly a factor of 100 higher, at 15Gy/h, at $\eta = 3.0$. The exponential increase in dose rate in the EE leads to pronounced differences in light yield loss in comparison to the EB.

In the simulation, the dose rate at dose maximum was calculated from the data in Fig. 11, according to the η position of the crystal, and normalised to the instantaneous luminosity in the detector. The dose rate at a particular depth in a crystal was calculated from the consequent dose rate at dose maximum using the normalised curves in Fig. 8.

The crystal light yield was calculated in real time at the LHC using equation (4). D was calculated at 1h intervals. These intervals were chosen to be short in comparison to the duration of an LHC fill of 14h. The values for D^0 and $R(t)$ were updated after each time interval and the process repeated until the end of the fill. Colour centre annealing was calculated between fills using the value of the annealing coefficient a . The process was repeated for one LHC year which was comprised of 3 LHC cycles each with 60 fills, a total of 4800h including the 10 days off between each cycle.

The light yield behaviour was calculated at six values of η : at 0 and 1.48 for EB, and at 1.6, 2.0, 2.5 and 2.9 for EE and for five values of the potential number of colour centres, D^{all} , in units of light yield loss, of 10, 20, 31.6, 40 and 50%. The calculations were performed at 1cm

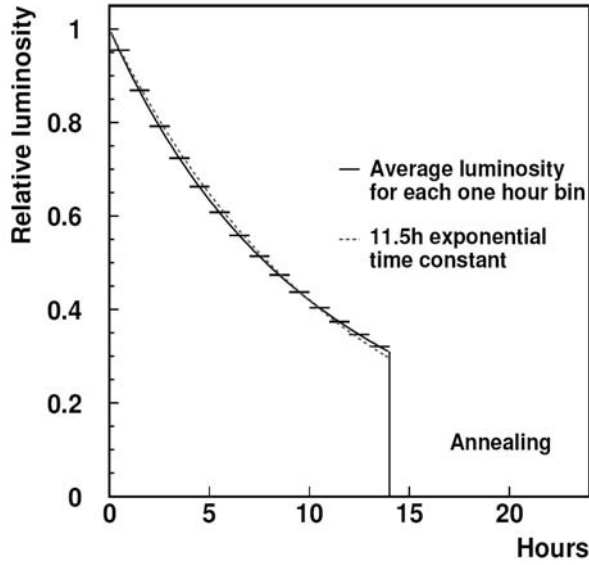


Figure 9.

The simulated LHC luminosity as a function of time (h). The luminosity decays with a form which is close to an exponential with a decay time of 11.5h (red dash line).

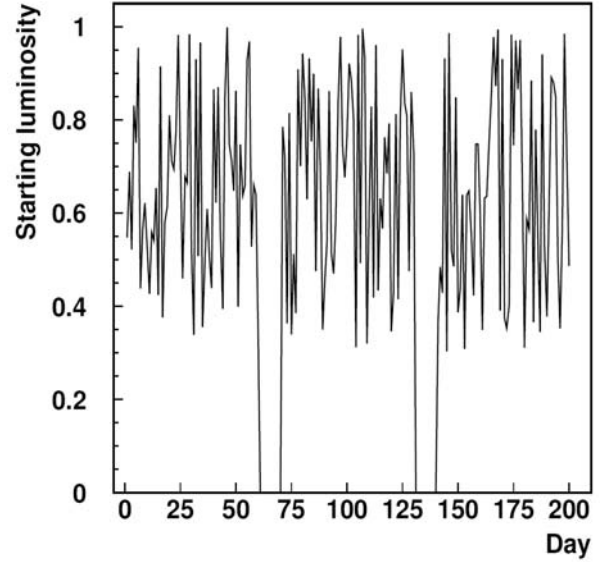


Figure 10.

Randomly generated fills for one year of LHC operation. The LHC year consists of 3 periods each with 60 fills separated by 10 days.

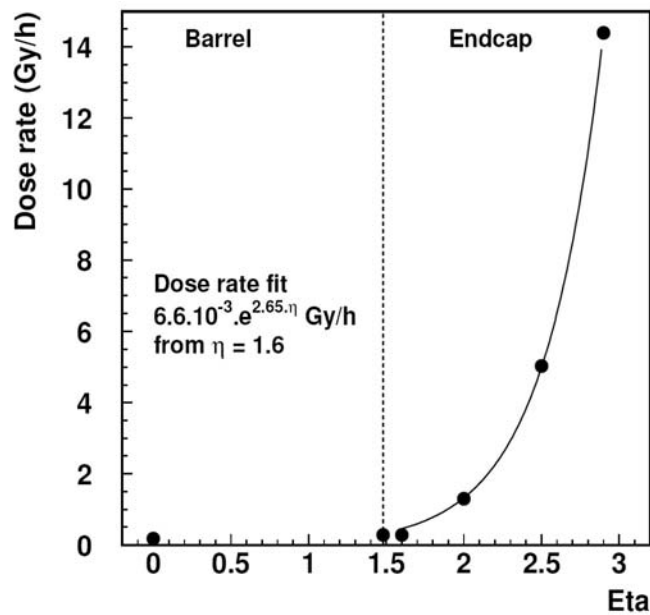


Figure 11.

The dose rate as a function of eta at the dose maximum in the crystals for a luminosity of $10^{34} \text{ cm}^{-2} \text{ s}^{-1}$.

steps along the length of the crystal from which a mean value for the light yield loss in the crystal was obtained for that time sampling.

The dose rate along the length of a crystal eight hours after the start of a fill, at $\eta = 2.5$, is shown in Fig. 12. The dose rate maximum is 1.5Gy/h, at a depth of 3cm in the crystal. The dose rate decreases to ~ 0.25 Gy/h at the end of the crystal. The corresponding density of colour centres along the crystal is shown in Fig. 13. The data are normalised to the light yield loss that would occur if that density of colour centres were present along the full length of a crystal. The net light yield loss averaged over these colour centre densities is 27.8%.

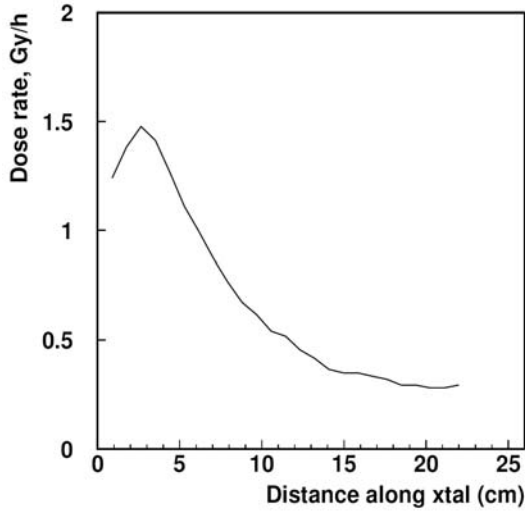


Figure 12.

The dose rate along a crystal 8h after the start of a fill, at $\eta = 2.5$.

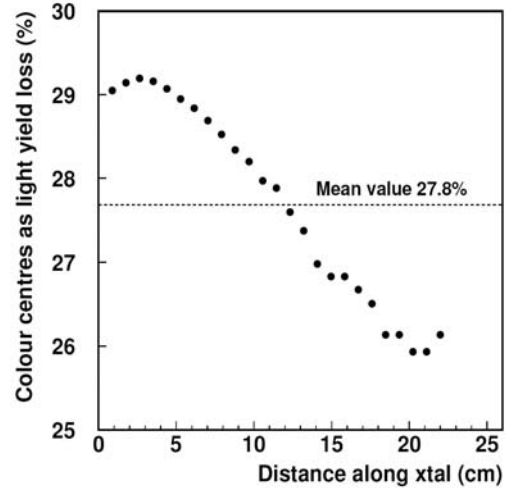


Figure 13.

The density of colour centres along a crystal 8h after the start of a fill, at $\eta = 2.5$. The average density of colour centres corresponds to a net light yield loss of 27.8%.

The average crystal light yield values, in hourly steps in real time at the LHC, are shown in Fig. 14 for low and high luminosity running at the LHC for maximum luminosities of 0.2 and $1.0 \cdot 10^{34} \text{ cm}^{-2} \text{ s}^{-1}$, respectively at $\eta = 0$ and at $\eta = 2.0$. The fill luminosity was randomly scaled by 30-100% to reflect fill to fill variations, as discussed in section 7. The same random scalings are applied to each fill for each of the luminosity cases (startup, low, high, and SLHC).

The data in Fig. 14 are for crystals with a D^{all} value of 31.6%, the most likely value for the number of potential colour centre sites for mass production BTCP crystals. The light yields are shown on the top row, together with a dashed line indicating the minimum light yield possible for this value of D^{all} , of 68.4%. The corresponding profiles of the LHC fills are shown on the bottom row normalised to $10^{34} \text{ cm}^{-2} \text{ s}^{-1}$. At low luminosity, the light yield losses in the EB at $\eta = 0$ are limited to $\sim 2\%$ whereas in the EE the losses are $\sim 15\%$ at $\eta = 2.0$. At high luminosity the losses at $\eta = 0$ have increased to $\sim 10\%$ and at $\eta = 2.0$ to 23.7%.

The structure of the light yield behaviour as a function of time is shown in more detail in Fig. 15 for high luminosity at $\eta = 2.0$. The peaks in the light yield reflect colour centre annealing, and the consequent light yield improvements, between LHC fills. The light yield, which is cal-

culated in hourly steps, can be weighted by the corresponding LHC luminosity to give the event normalised average light yield. The event normalised average light yield is indicated by the solid line in Fig. 15 and has a value of 73.6% for the crystal for one year of LHC running (excluding LHC off periods).

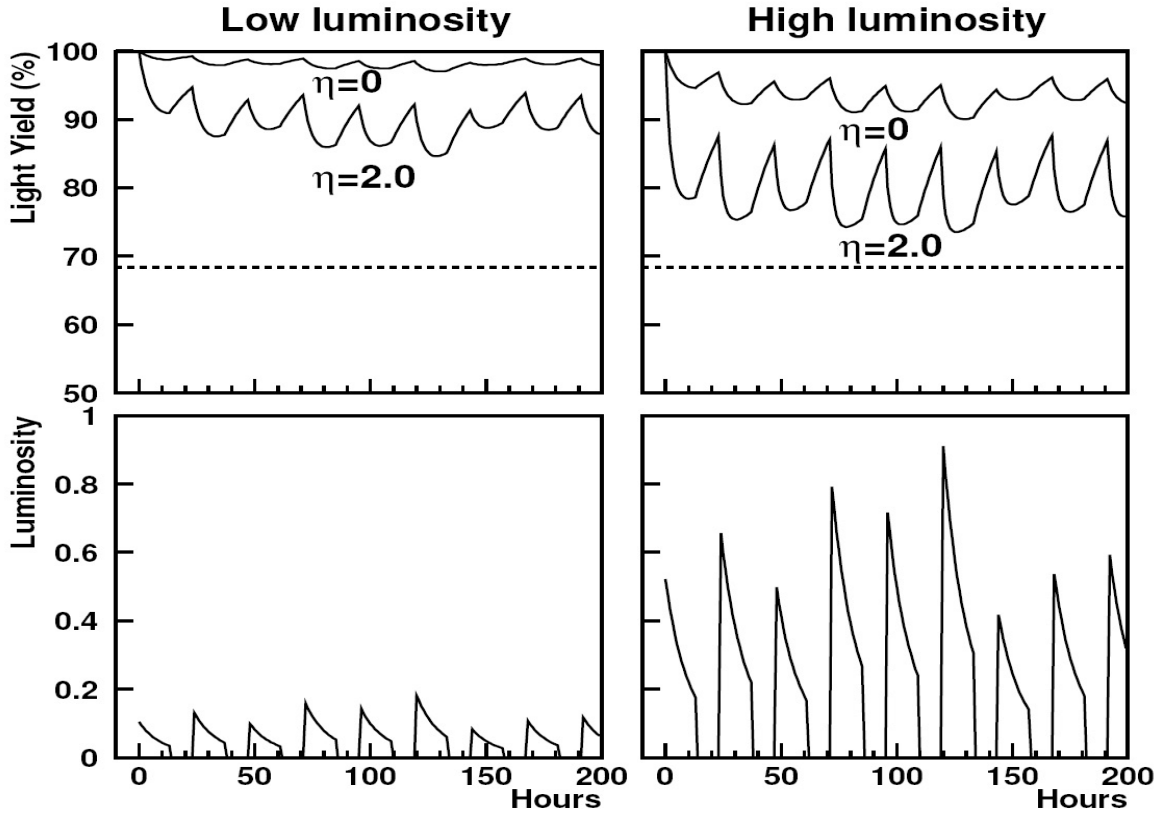


Figure 14.

Top row: the crystal light yield (%) as a function of time at the LHC at $\eta = 0$ and $\eta = 2.0$ for low and high luminosity running at the LHC, for a typical crystal with $D^{all} = 31.6\%$.

Bottom row: the corresponding luminosity of the LHC fills as a function of time normalised to $10^{34} \text{ cm}^{-2} \text{ s}^{-1}$.

The behaviour of the light yield in Fig. 15 shows that the average light yield at $\eta = 2.0$ is nearly established after only two hours of LHC operation in the first fill of the year. Fig. 16 shows the hour by hour changes in light yield as a function of time during the fill, for all 180 fills in a year. The largest changes in crystal light yield take place in the first two to three hours of a fill and vary in magnitude from $\sim 4\%$ to $\sim 1\%$ from one hour to the next. Thereafter, colour centre creation is balanced by colour centre annealing, as the luminosity decreases, and after ~ 10 hours the light yield starts to increase by $\sim 0.4\%$ for each hour of elapsed time. The distribution of the hourly light yield changes is shown in Fig. 17.

The simulation has been repeated for annealing times of 30, 40 and 100h, instead of 18.55h, but with the same colour centre creation coefficient, b , as obtained for BTCP crystal 4005. At high luminosity the magnitude of light yield change in the first hour of a fill reaches 3.5%, instead of $\sim 4\%$, for a 30h annealing time. This reduces to $\sim 3\%$ for a 40h annealing time and to $\sim 1.5\%$ for a 100h annealing time.

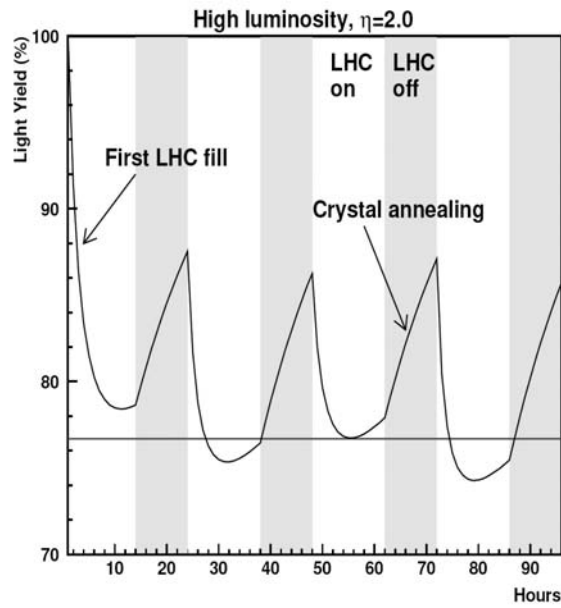


Figure 15.

The light yield response during the first four LHC fills at high luminosity at $\eta = 2.0$ for a crystal with $D_{all} = 31.6\%$. The vertical yellow bands indicate the 10h periods between fills when the LHC is off. The horizontal line indicates the event weighted mean crystal light yield of 76.3% during the LHC fills.

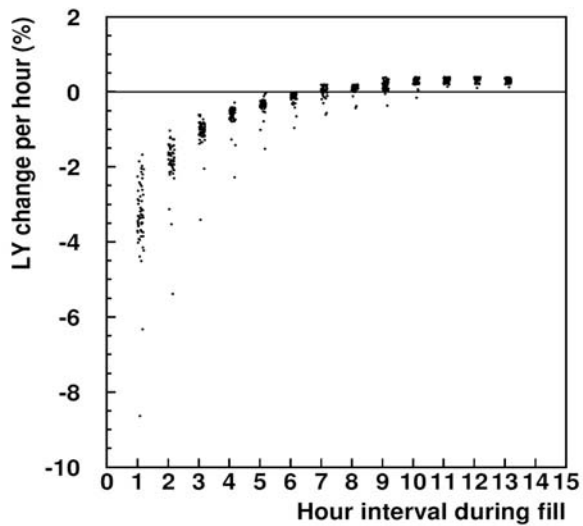


Figure 16.

Light yield change per hour, as a function of the time interval in the fill taken over all fills, at $\eta = 2$ at high luminosity, for a crystal with $D_{all} = 31.6\%$.

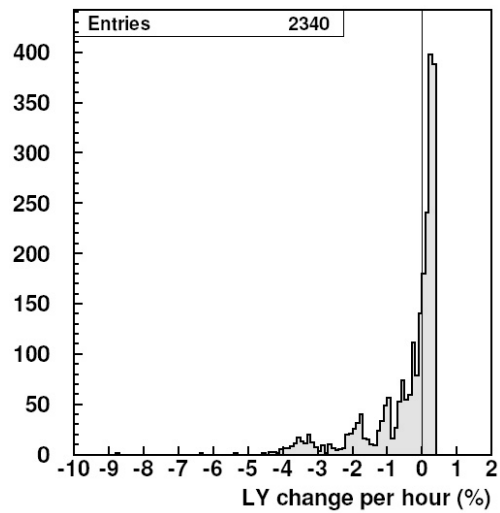


Figure 17.

The distribution of the light yield changes per hour, at $\eta = 2$, over all fills, at high luminosity, for a crystal with $D_{all} = 31.6\%$.

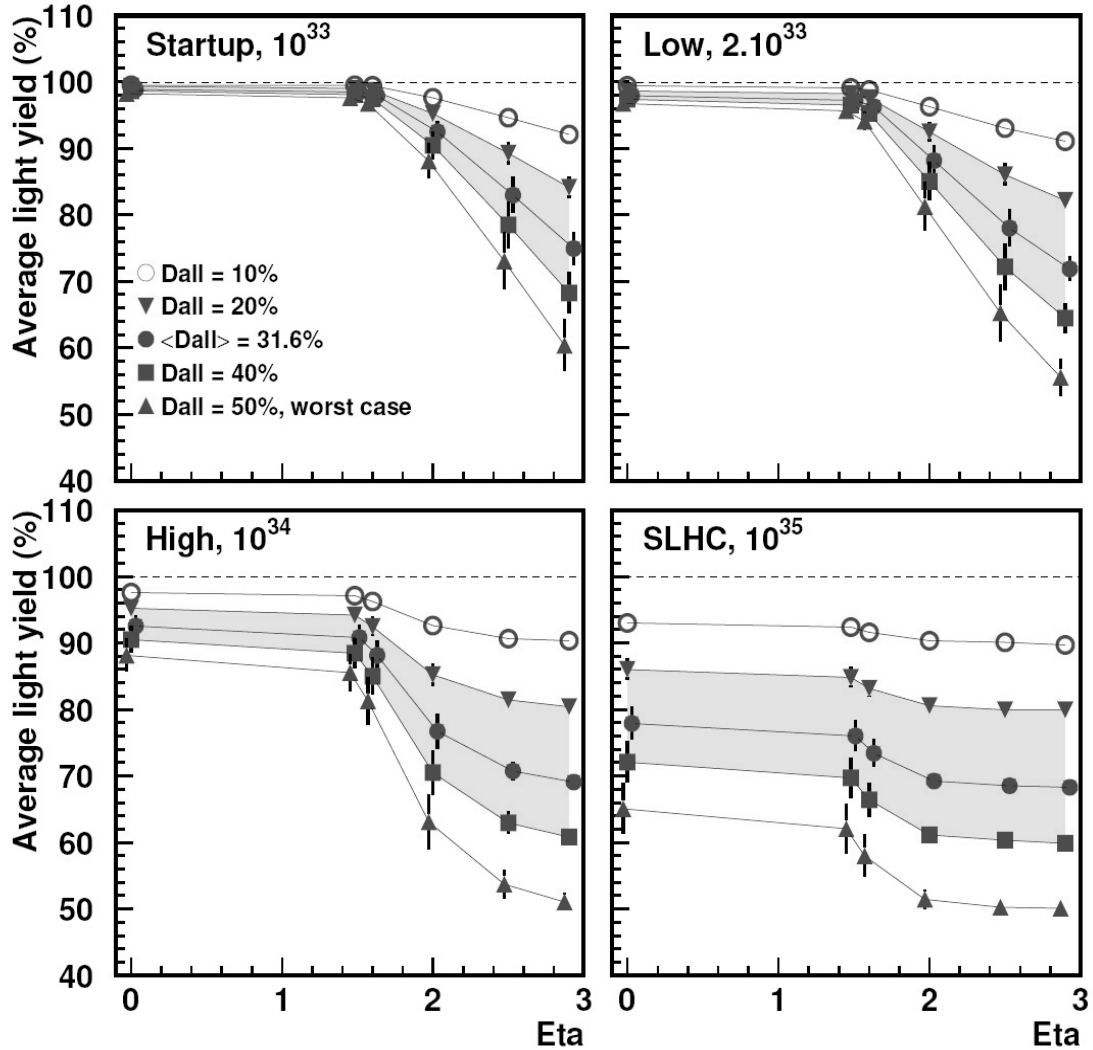


Figure 18.

The event weighted average crystal light yield as a function of η for startup, low, high and SLHC running during fills at the LHC. Crystal light yields for 5 densities of potential colour centres are plotted in each view. The highlighted regions indicates the ± 1 sigma band for the most likely potential colour centre density in the crystals.

It is intended to follow and correct for light yield changes at the 0.2% level. For light yield changes of 4% over an elapsed time of one hour corrections would need to be made every 3 minutes to the data. This could be carried out by a possible combination of more frequent laser monitoring, in the parts of the ECAL where changes of such magnitude are taking place, and by interpolating between laser runs if a more frequent laser monitoring cycle is not possible.

Laser pulse height distributions measured at the testbeam have widths of $\sim 0.5\%$ [17]. The mean is measured to within 0.1% with less than 100 pulses. At a laser trigger rate of 100Hz at the LHC only one second is required for each laser monitoring region in the ECAL. However, due to hardware constraints, it is expected that the laser monitoring system can only cover one region of ECAL in 25 seconds. The 72 regions of EB and the 18 regions of the EE will require a total of 30 and 7.5 minutes respectively for complete laser monitoring coverage.

The long duration of the laser monitoring cycle over the ECAL indicates that interpolation between laser data points at different times will be necessary to adequately correct for the interim light yield changes.

The event weighted mean crystal light yield as a function of η is shown in Fig. 18 for the four run setups at the LHC: startup, low, high and Super LHC (SLHC) with nominal starting fill luminosities of 10^{33} , 2.10^{33} , 10^{34} and 10^{35} $\text{cm}^{-2} \text{s}^{-1}$, respectively. The light yields for crystals with five levels of potential colour centre density, D^{all} , have been displayed with values of 10, 20, 31.6, 40 and 50%. The error bars on the plots correspond to the r.m.s changes in light yield during one year of LHC operation (LHC fill periods only).

The values of D^{all} between 20 and 40% approximately represent the ± 1 sigma band for the most likely densities of potential colour centres in the crystals with the mean value of D^{all} of 31.6% taken from Fig. 6. The values for the event weighted mean light yields are listed in Table 2 for crystals with $D^{all} = 31.6\%$ for the five eta regions in the simulation, for startup, low, high and SLHC luminosities.

At startup and low luminosity the light yield losses in the barrel ($\eta < 1.48$) are less than 2.1% for a crystal with $D^{all} = 31.6\%$. The losses rise linearly in the EE as a function of eta to $\sim 25\%$ at $\eta = 2.9$. At high luminosity the average losses in the EB are between 7.5 and 9.1%. In the EE, colour centre creation starts to saturate as a function of eta. The light yield loss flattens and is 30.9% at $\eta = 2.9$ which is close to the maximum possible light yield loss for crystals with $D^{all} = 31.6\%$. At SLHC the light yield losses in EB are between 22 and 26.5% and are saturated at nearly all eta values in the EE at 31.6%.

Table 2: Mean loss of light (%) as a function of eta for the four LHC running conditions, for crystals with $D_{all} = 31.6\%$

Eta	Startup $10^{33} \text{ cm}^{-2} \text{ s}^{-1}$	Low $2.10^{33} \text{ cm}^{-2} \text{ s}^{-1}$	High $10^{34} \text{ cm}^{-2} \text{ s}^{-1}$	SLHC $10^{35} \text{ cm}^{-2} \text{ s}^{-1}$
0.0	1.1	2.1	7.5	22.0
1.48	1.5	2.8	9.1	23.9
1.6	2.0	3.7	11.8	26.5
2.0	7.5	11.8	23.3	30.7
2.5	17.0	22.0	29.2	31.4
2.9	25.0	28.1	30.9	31.6

The simulation has been repeated for annealing times of 30, 40 and 100h, instead of 18.55h, but with the same colour centre creation coefficient, b , as obtained for BTCP crystal 4005. At high luminosity the event weighted mean light yield losses (for a crystal with $D_{all} = 31.6\%$ at $\eta = 2.0$) are 26%, 27.2% and 29.6% respectively, in comparison to 23.3% in Table 2. For annealing times which are longer than $\sim 40\text{h}$ essentially all the available colour centres remain populated from one fill to the next.

9: Monitoring the crystal light yield at the LHC

The CMS ECAL laser monitoring system is used to follow the change in light yield due to colour centre formation in the crystals. A laser light source of 440nm is used to monitor the transparency of the crystal near the emission peak of PbWO_4 . Changes in the laser signal have been shown to follow changes in the scintillation signal response from particles [4]. The ratio of the changes is commonly referred to as the ‘R’ parameter where $R = \frac{\Delta \text{particle signal}}{\Delta \text{monitoring signal}}$. It is hoped that crystal production will show little variation in R , otherwise the value of R would become another calibration constant and would have to be measured for each of the 75848 crystals in the ECAL.

The range within which R can vary from crystal to crystal depends on the energy resolution targets for the detector and the amplitude of the corrections required during LHC operation. It can be shown that the error on normalising the energy of the particle signal is given by:

$$\frac{\sigma_E}{E} = \frac{\Delta LY}{\langle LY \rangle} \cdot \frac{\sigma_R}{R} \quad (6)$$

where σ_E/E is the fractional error on the energy measurement, $(\Delta LY)/(\langle LY \rangle)$ is the fractional r.m.s. change in crystal light yield and σ_R/R is the fractional variation on R .

Fig. 19 shows the variation of $(\Delta LY)/(\langle LY \rangle)$ as a function of η for the four LHC run setups. The plots show the limits (dashed horizontal lines) of the monitoring system to follow the light yield variations with sufficient precision if the impact on the energy resolution, σ_E/E , is to be less than 0.3%.

The top and bottom dashed lines in Fig. 19 are for values of σ_R/R of 6% and 16%, respectively. This range of values for R was found for a small and a larger group of crystals at the GIF facility at CERN, respectively [18]. It can be seen from Fig. 19 that in order for the energy resolution to be measured with sufficient accuracy over all crystal types, and over all likely LHC scenarios, σ_R/R must be less than 6%.

The fractional variation in light yield during LHC operation is listed in Table 3 for crystals with $D^{all} = 31.6\%$ for the five eta regions in the simulation, for startup, low, high and SLHC luminosities. The largest fractional changes in each column are indicated by bold text. The largest changes are in the EE for startup, low and high luminosities. However at high luminosity colour centre saturation can be seen in the EE beyond $\eta = 2.0$. The changes are less than 2% in comparison to 3.4% at $\eta = 2.0$. At SLHC the largest changes are in EB at 3.1% while in the EE the saturation of colour centre creation limits the changes to below 1.3% beyond $\eta = 1.6$.

It is important to note that the reference crystal light yield should be the event normalised mean light yield during LHC operation $\langle LY \rangle$ and not the light yield measured prior to LHC operation, for example at test beams. The error due to the lever arm brought about by correcting for light yield losses of 30% with respect to test beam measurements would dominate the relative changes in light yield, of typically 4% or less, at the LHC itself and would set proportionately tighter requirements for the variation in R .

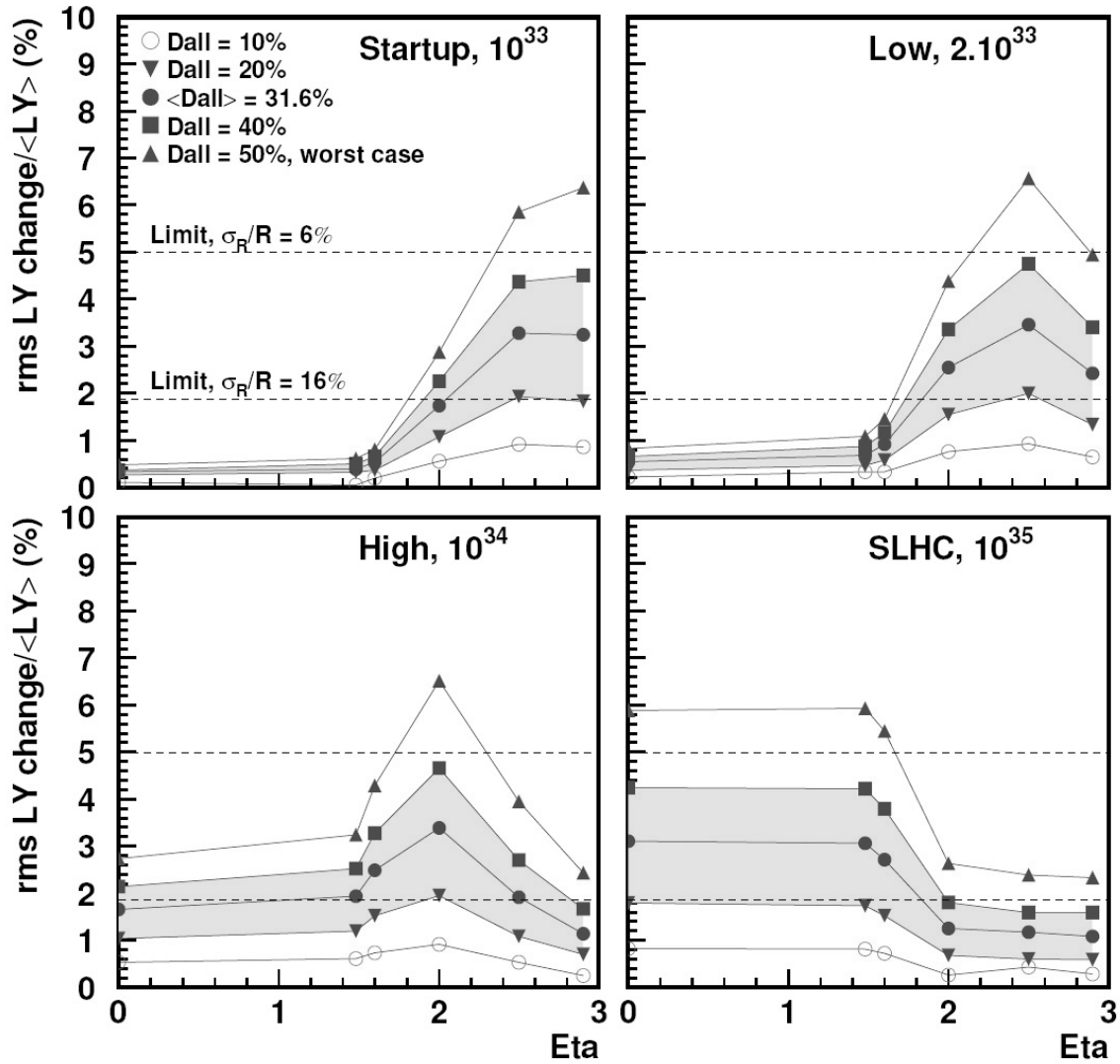


Figure 19.

The percentage light yield change as a function of η for startup, low, high and SLHC periods at LHC. The highlighted regions indicate the ± 1 sigma band for the most likely colour centre density in the crystals. The top and bottom dashed lines in each view indicate the limitations of the monitoring system for variations in 'R' of 6 and 16% respectively.

The simulation has been repeated for annealing times of 30, 40 and 100h but keeping the colour centre creation dynamics the same as for BTCP crystal 4005. At high luminosity the fractional variations of light yield (for a crystal with $D_{all} = 31.6\%$ at $\eta = 2.0$) are 2.9%, 2.6% and 2.0% respectively, in comparison to 3.4% in Table 3.

The reductions in the r.m.s. light yield variation for the 30 and 40h annealing times would permit a 25% increase in σ_R/R from 6% to 7.5% for such crystals to be adequately monitored at high luminosity. However, at present, there is no confirmation that crystals will conform to such bounds and it is likely that in-situ values of R will have to be found for each crystal during LHC operation.

Table 3: The fractional variation of light yield (%) as a function of eta for the four LHC running conditions, for crystals with $D_{\text{all}} = 31.6\%$

Eta	Startup $10^{33} \text{ cm}^{-2} \text{ s}^{-1}$	Low $2 \cdot 10^{33} \text{ cm}^{-2} \text{ s}^{-1}$	High $10^{34} \text{ cm}^{-2} \text{ s}^{-1}$	SLHC $10^{35} \text{ cm}^{-2} \text{ s}^{-1}$
0.0	0.3	0.5	1.7	3.1
1.48	0.4	0.7	1.9	3.1
1.6	0.5	0.9	2.5	2.7
2.0	1.7	2.6	3.4	1.3
2.5	3.3	3.5	1.9	1.2
2.9	3.3	2.4	1.1	1.1

The r.m.s. light yield variation of 2%, for the case of the 100h annealing time, is largely due to the changes in the average LHC luminosity over longer periods of time, of more than 48-72h, corresponding to 3 or more fills. These contribute to long range changes to the average light yield of the crystal.

Changes of the LHC luminosity, over longer time periods (weeks and months), will require a re-definition of the average light yield in the crystals about which to make monitoring corrections.

10: ECAL noise levels and the ECAL trigger system

In the EB the mean light yield losses are less than 10% for startup, low and high luminosity operation. These light yield losses will give rise to pro rata increases for the EB noise levels. In the EE, the mean light yield loss is $\sim 29\%$ at high luminosity at $\eta = 2.5$, the limit for high resolution physics. This light yield loss imposes proportionately tighter noise targets for the EE electronics design, in order to meet the final ECAL operational noise targets.

The span of the light yield change during a fill is $\sim 10\%$ in the EE, at $\eta = 2.0$. The light yield changes cannot be accommodated in real time by the front end trigger electronics. This will introduce proportional biases to the calculated energies seen by the crystals during a fill, particularly in the first one to two hours, which correspond to the highest luminosities and highest event rates within the fill (section 8).

11: Other crystal behaviour

The dynamics of colour centre creation and annihilation vary from one crystal to another. The crystal used in this simulation (BTCP #4005) was assumed to anneal back to its initial state with a single exponential recovery time. In fact, as can be seen in Fig. 1, the recovery is not complete and a 1% residual light yield loss remains, which represents $\sim 30\%$ of the total light yield loss.

Many crystals show such partial recovery. This is thought to be due to very long annealing time constants for some types of colour centre trap. The consequences for ECAL operation are twofold. Firstly, such crystals will have a specific level of colour density associated with the

long lived traps and these will contribute to the average light yield loss over long periods of time.

Secondly, the traps which have shorter annealing time constants will represent a smaller population of the total number of potential colour centres in the crystal. The r.m.s. light yield variations will be proportionately less in such crystals, giving rise to more stable ECAL operation.

Some crystals (particularly those from SIC) show quick colour centre creation and very long (>100h) annealing times. Essentially all the available colour centres will be activated in such crystals. However the r.m.s. light yield variations should be small with correspondingly less stringent demands on the laser monitoring system.

12: Conclusions

A simulation has been carried out to quantify the changes in light yield to be expected from crystals in the CMS ECAL during LHC operation. At startup, low and high luminosities EB light yield losses are less than 10%, whereas in EE the losses rise to ~29% at high luminosity at $\eta = 2.9$.

The fractional light yield changes in the ECAL are such that adequate laser monitoring of colour centre creation can only be guaranteed if the spread in the 'R' parameter for crystals is less than 6%.

It is likely that such an 'R' parameter will have to be evaluated in-situ at the LHC for each crystal in the ECAL before global monitoring corrections can be applied with confidence.

The rate of light yield change in the first 2 hours of an LHC fill is at the level of 4% per hour at high luminosity, at $\eta = 2.0$, which corresponds to the central region for high resolution physics in the EE. These changes will be the most challenging for the laser monitoring system to follow and may require that the laser monitoring system is used preferentially in some parts of the ECAL to adequately track the light yield changes, in balance to the changes occurring elsewhere.

References

- [1] CMS ECAL Technical Design Report, CERN/LHCC 97-33, 1997.
- [2] 'Energy resolution of the CMS ECAL barrel super-module using MGPA electronics', G. Dewhirst, R. Bruneliere, CMS Note RN 2004/004.
- [3] 'Systematic study of the PbWO₄ crystal short term instability under irradiation', A.N. Annenkov et al., CMS Note 1997/008, 1997.
- [4] 'The monitoring system for CMS-ECAL', J. Rander, 8th International Conference on Calorimetry in High Energy Physics, Lisbon 1999, p423.
'Performance of the monitoring light source for the CMS Lead Tungstate Crystal Calorimeter', L. Zhang et al., IEEE, Vol 52, No 4, Aug 2005.
- [5] 'High-energy proton induced damage in PbWO₄ calorimeter crystals', M. Huhtinen et al., NIM-A 545 (2005) 63-87.
- [6] 'On optical bleaching of barium fluoride crystals', D. Ma and R.Y. Zhu, NIM-A 332 (1993) 113-120.
- [7] 'A study on the radiation hardness of lead tungstate crystals', R.Y.Zhu et al., IEEE Trans. Nucl. Sci., Vol 45 (1998) 686.

- R.Y. Zhu, IEEE Trans. Nucl. Sci., Vol 44 (1997) 468.
'Radiation damage kinetics in PbWO₄ crystals', A.N. Annenkov et al., CMS Note 1997/009.
- [8] 'PbWO₄ Crystals Radiation Hardness Test Setup at the CERN General Irradiation Facility', J-P. Peigneux et al., CMS NOTE-1999/061.
- [9] 'GIF Status report', P. Rebecchi, ECAL Technical Coordination Group meeting, 19.2.2002.
- [10] E. Auffray, ECAL Detector Performance Group meeting, 16.3.2004, EB batch S4, BTCP crystals 18801-22090.
S. Baccarro, ECAL Detector Performance Group meeting, 21.9.2004, SIC crystals 2602-2616 from January 2004.
- [11] 'Improvement of Several Properties of Lead Tunstate Crystals with Different Doping Ions', E Auffray et al., CMS Note 1997/054.
- [12] 'Various results on Endcap crystals', E. Auffray, ECAL Detector Performance Group meeting, 11.6.2002, BTCP crystals from 2368-2467, 2001.
E. Auffray, private communication, BTCP crystals 2469-2532, 2003, SIC crystals 2569-2648, January, 2004.
- [13] 'Status of New Technology Development in Bogoroditsk', P. Lecoq, CMS week plenary, Catania, Italy, June 2001, from BTCP preproduction (6000 crystals), final batches 11-14.
- [14] Hybrid Photomultiplier (HPMT), Delft Electronics Products B.V. (DEP), The Netherlands.
- [15] 'Luminosity considerations for the LHC', K. Eggert et al., CERN AT/94-04, LHC Note 263.
The LHC design report, Volume 1, Chapter 3, Layout and performance.
- [16] Private communication, O. Bruening, LHC group, CERN.
- [17] Private communication, C. Seez, L. Malgeri, 7.10.2004.
- [18] 'A Study of the Monitoring of Radiation Damage to CMS ECAL Crystals, performed at X5-GIF, G. Davies et al., J. Phy. G: Nucl. Part. Phys. 26 (2000) 1735-1749, and CMS Note 2000/020,